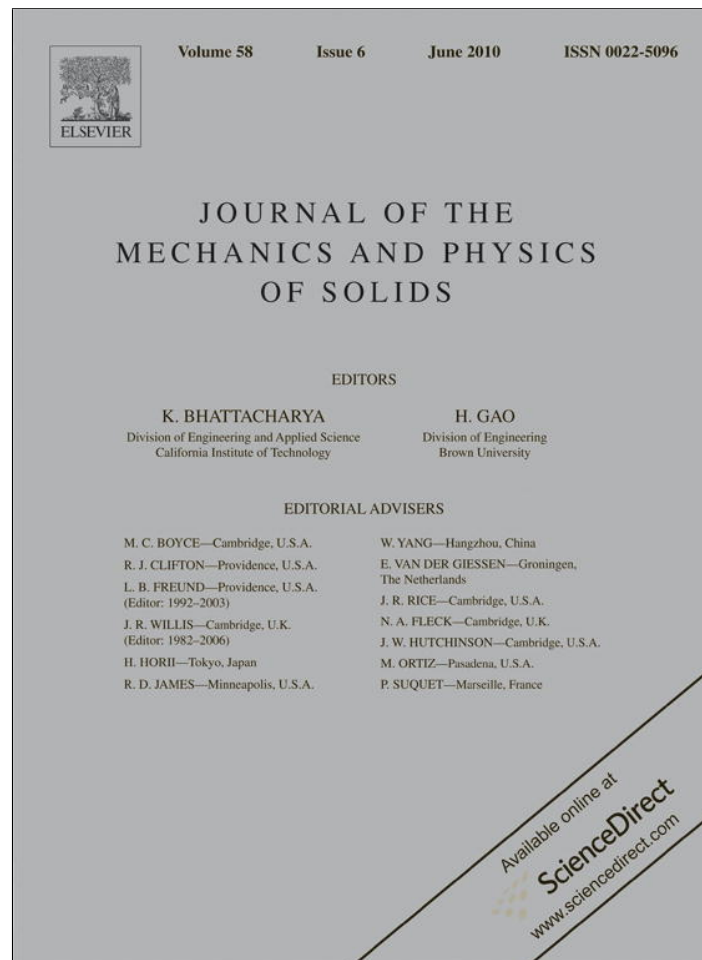


Provided for non-commercial research and education use.
Not for reproduction, distribution or commercial use.



This article appeared in a journal published by Elsevier. The attached copy is furnished to the author for internal non-commercial research and education use, including for instruction at the authors institution and sharing with colleagues.

Other uses, including reproduction and distribution, or selling or licensing copies, or posting to personal, institutional or third party websites are prohibited.

In most cases authors are permitted to post their version of the article (e.g. in Word or Tex form) to their personal website or institutional repository. Authors requiring further information regarding Elsevier's archiving and manuscript policies are encouraged to visit:

<http://www.elsevier.com/copyright>



Contents lists available at ScienceDirect

Journal of the Mechanics and Physics of Solids

journal homepage: www.elsevier.com/locate/jmps

Crack in a 2D beam lattice: Analytical solutions for two bending modes

Michael Ryvkin*, Leonid Slepyan

School of Mechanical Engineering, Tel Aviv University, Israel

ARTICLE INFO

Article history:

Received 4 November 2009

Received in revised form

19 March 2010

Accepted 27 March 2010

Keywords:

A. Fracture toughness
B. Elastic material
C. Integral transforms
Asymptotic analysis
Functionally invariant solutions

ABSTRACT

We consider an infinite square-cell lattice of elastic beams with a semi-infinite crack. Symmetric and antisymmetric bending modes of fracture under remote loads are examined. The related long-wave asymptotes corresponding to a continuous anisotropic bending plate are also considered. In the latter model, the symmetric mode is characterized by the square-root type singularity, whereas the antisymmetric mode results in a hyper-singular field. A solution for the continuous plate with a finite crack is also presented. These closed-form continuous solutions describe the fields in the whole plane. The main goal is to establish analytical connections between the 'macrolevel' state, defined by the continuous asymptote of the lattice solution, and the maximal bending moment in the crack-front beam, that is, to determine the resistance of the lattice with an initial crack to the crack advance. The solutions are obtained in the same way as for mass-spring lattices. Considering the static problems we use the discrete Fourier transform and the Wiener-Hopf technique. Monotonically distributed bending moments ahead of the crack are determined for the symmetric mode, and a self-equilibrated transverse force distribution is found for the antisymmetric mode. It is shown that in the latter case only the crack-front beam resists to the fracture development, whereas the forces in the other beams facilitate the fracture. In this way, the macrolevel fracture energy is determined in terms of the material strength. The macrolevel energy release is found to be much greater than the critical strain energy of the beam, especially in the hyper-singular mode. In both problems, it is found that among the beams surrounding the crack the crack-front beam is maximally stressed, and hence its strength defines the strength of the structure.

© 2010 Elsevier Ltd. All rights reserved.

1. Introduction

Increasing interest in cellular materials has resulted, in particular, in the development of fracture mechanics of materials with a microstructure. In the present paper, two bending modes of fracture of a 2D periodic lattice composed of rigidly connected Euler-Bernoulli beams are considered analytically. Plane problems of such lattices were studied in a number of works.

A comprehensive review of the subject is given in the monograph by Gibson and Ashby (1997). The lattice fracture toughness was determined in terms of the material strength by different methods. Some authors have employed the approach suggested by Ashby (1983), where the stress state of the crack-front beam was determined based on the

* Corresponding author. Tel.: +972 3 640 8130; fax: +972 3 640 7334.
E-mail address: arikr@eng.tau.ac.il (M. Ryvkin).

near-the-crack-tip singular stress distribution in the related homogeneous model (Maiti et al., 1984; Fleck and Qiu, 2007). The stress field in a finite lattice with a crack has also been evaluated using the finite element method (Schmidt and Fleck, 2001; Fleck and Qiu, 2007; Huang and Gibson, 1991; Choi and Sankar, 2005; Quintana Alonso and Fleck, 2007). An infinite bending beam lattice with a finite crack was considered using a combined analytical–numerical method based on the discrete Fourier transform (Lipperman et al., 2007, 2008, 2009). In all of the aforementioned works, the plane problems for the bending beam lattices has been investigated. Bending deformation of such a lattice resting on elastic supports with several elements missing was considered by Fuchs et al. (2004). Nuller and Ryvkin (1980) employed the discrete Fourier transform in the bending of a lattice subjected to a transverse force.

Dynamic and quasi-static crack growth in simpler mass–spring square and triangular lattices were analytically considered in many works beginning from Slepyan (1981). The technique and main results are presented in Slepyan (2002). A nonzero-bond-density lattice fracture was studied in Slepyan (2005) and a lattice with a low-density waveguide was considered in Mishuris et al. (2009). These lattices are characterized by a single force–displacement relation, and this allows the Wiener–Hopf technique to be straightforwardly used. In the general case of a beam lattice, where the bonds resist extension, shear, bending and torsion, the crack problem is much more complicated, and no analytical solution has yet been obtained.

In the present paper, a partial case of the general fracture problem for a beam lattice is analytically considered, where the Wiener–Hopf technique can be used. Namely, we consider a two-dimensional square lattice under bending. The main goal is the crack resistance determination in terms of the ‘macrolevel’ energy release and the lattice beam strength. Based on the linear theory, it is assumed that each node has three degrees of freedom: the transverse displacement and rotations about two axes. There are no in-plane forces, and the classical Euler–Bernoulli beams resist to the transverse forces and bending moments; torsion moments are neglected. The beams form a regular square lattice; they are rigidly connected at the lattice nodes. A straight semi-infinite crack is assumed to exist. The strain of the lattice is caused by the action of a remote loading. We assume that the beams break under the critical bending moment.

Due to the symmetry a lattice half-plane can be considered with the boundary at the crack line. For the analytical technique used below the conditions at this boundary are important. In our case, two energy pairs exist at the half-plane boundary: the transverse force acting on the half-plane with the corresponding displacement, and the bending moment–rotation about the crack line. The latter pair corresponds to the symmetric fracture mode (the displacements are symmetric with respect to the crack line) with no transverse force on the crack line, whereas for the antisymmetric mode there is no bending moment on the crack line. In both cases, the discrete Fourier transform allows us to reduce the problem to a single Wiener–Hopf type equation which is then solved analytically.

In addition to the mode-dependent boundary conditions on the crack line, the general solution is subjected to the *vanishing stress condition* at infinity. This means that the bending moment and the transverse force must tend to zero as the distance from the crack front tends to infinity. The derivation of Green’s function for the lattice half-plane is based on the causality principle, namely, it is assumed that the relation between the displacement (rotation) and the transverse force (bending moment) applied on the crack line corresponds to the local loading, and no remote forces influence this relation. This allows a proper factorization of the Green function F -transform to be performed. The causality principle, however, does not concern the Wiener–Hopf equation’s right-hand side introduced to reflect the remote loads action (in this connection, see Slepyan, 2002, Section 11.5.1). We call a finite strain-energy-density solution, satisfying these conditions, the physically acceptable solution.

The paper plan is as follows. First, we consider general solutions for the lattice half-plane and crack-related functionally invariant solutions for the corresponding continuous domain. The lattice solution is expressed in terms of the discrete Fourier transform on m ($m=0, \pm 1, \dots$ is the crack line discrete coordinate), whereas the explicit continuous solution is presented in terms of the original continuous coordinates. Then the symmetric-mode solutions are derived. The distribution of bending moments in the beams ahead of the crack is found as a function of the far-field energy release rate or the corresponding moment intensity factor, and the continuous approximation of the lattice deformation in the whole plane is finally determined. Further, the related solutions for the antisymmetric mode are derived. Finally, a brief discussion is presented.

2. Formulation and general solution

2.1. The lattice and equilibrium equations

Consider an infinite uniform square-cell lattice (a grillage) consisting of Euler–Bernoulli beams rigidly connected at the nodes. The beams, of length a and of bending stiffness EI (E is the elastic modulus and I is the moment of inertia), are located along the lines $x=am$ and $y=an$ ($m, n=0, \pm 1, \pm 2, \dots$) of the Cartesian coordinate system (x, y, z) , Fig. 1. The torsion stiffness of the beam is neglected.

The state of the lattice for the case of bending deformations considered herein is completely defined by three generalized displacements of the nodes: the transverse displacement, $w_{m,n}$ (displacement in z -direction), and the rotations, $\theta_{m,n}^x$ and $\theta_{m,n}^y$, Fig. 2. The bending moment and transverse force in the beam between the nodes (m, n) and $(m+1, n)$ are

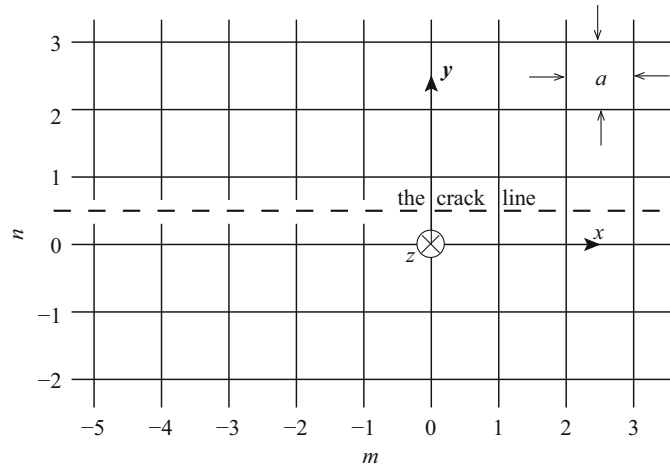


Fig. 1. The lattice with a semi-infinite crack. The beams of bending stiffness EI are rigidly connected at the nodes.

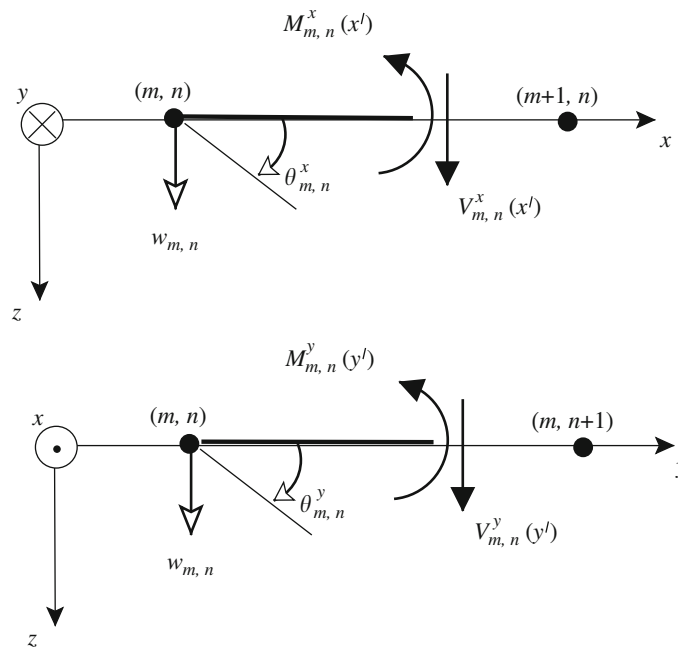


Fig. 2. Positive directions of the forces, moments, rotations and displacements.

denoted as $M_{m,n}^x(x')$, $V_{m,n}^x(x')$, respectively ($x = am + x', 0 < x' < a, y = an$), and those in the beam between the nodes (m, n) and $(m, n+1)$ are denoted as $M_{m,n}^y(y')$, $V_{m,n}^y(y')$, respectively ($x = am, y = an + y', 0 < y' < a$).

The positive directions are shown in Fig. 2. These quantities can be expressed in terms of the displacements and rotations of the beam nodes as follows:

$$V_{mn}^x(x') = \frac{6EI}{a^3} [2(w_{m+1,n} - w_{m,n}) - a(\theta_{m+1,n}^x + \theta_{m,n}^x)],$$

$$M_{m,n}^x(x') = \frac{2EI}{a^3} [3(2x' - a)(w_{m+1,n} - w_{m,n}) + (a - 3x')a\theta_{m+1,n}^x + (2a - 3x')a\theta_{m,n}^x],$$

$$V_{mn}^y(y') = \frac{6EI}{a^3} [2(w_{m,n+1} - w_{m,n}) - a(\theta_{m,n+1}^y + \theta_{m,n}^y)],$$

$$M_{m,n}^y(y') = \frac{2EI}{a^3} [3(2y' - a)(w_{m,n+1} - w_{m,n}) + (a - 3y')a\theta_{m,n+1}^y + (2a - 3y')a\theta_{m,n}^y]. \tag{1}$$

Thus, the equilibrium equations

$$V_{m,n}^x(0) + V_{m,n}^y(0) - V_{m-1,n}^x(a) - V_{m,n-1}^y(a) = 0,$$

$$M_{m,n}^x(0) - M_{m-1,n}^x(a) = 0,$$

$$M_{m,n}^y(0) - M_{m-1,n}^y(a) = 0 \tag{2}$$

being expressed in terms of the node displacements have the form

$$2(w_{m-1,n} + w_{m+1,n} + w_{m,n-1} + w_{m,n+1} - 4w_{m,n}) + a(\theta_{m-1,n}^x - \theta_{m+1,n}^x + \theta_{m,n-1}^y - \theta_{m,n+1}^y) = 0, \tag{3}$$

$$3(w_{m-1,n} - w_{m+1,n}) + a(\theta_{m-1,n}^x + \theta_{m+1,n}^x + 4\theta_{m,n}^x) = 0, \tag{4}$$

$$3(w_{m,n-1} - w_{m,n+1}) + a(\theta_{m,n-1}^y + \theta_{m,n+1}^y + 4\theta_{m,n}^y) = 0. \tag{5}$$

2.2. General solutions

The discrete Fourier transform on m

$$f^F = \sum_{m=-\infty}^{\infty} f_m \exp(ikm) \tag{6}$$

converts the 2D problem (3)–(5) into a 1D problem in the F -transform space

$$(4\cos k - 8)w_n^F + 2w_{n-1}^F + 2w_{n+1}^F + a(2i\sin k \theta_n^{xF} + \theta_{n-1}^{yF} - \theta_{n+1}^{yF}) = 0, \tag{7}$$

$$+ 3i\sin k w_n^F + a(\cos k + 2)\theta_n^{xF} = 0, \tag{8}$$

$$3(w_{n-1}^F - w_{n+1}^F) + a(\theta_{n-1}^{yF} + \theta_{n+1}^{yF} + 4\theta_n^{yF}) = 0. \tag{9}$$

Referring to (8), system (7)–(9) becomes

$$\left(4\cos k - 8 + \frac{6\sin^2 k}{\cos k + 2}\right)w_n^F + 2w_{n-1}^F + 2w_{n+1}^F + a(\theta_{n-1}^F - \theta_{n+1}^F) = 0, \tag{10}$$

$$3(w_{n-1}^F - w_{n+1}^F) + a(\theta_{n-1}^F + \theta_{n+1}^F + 4\theta_n^F) = 0. \tag{11}$$

Hereafter the superscript y is omitted; we use notations θ, M, V instead of θ^y, M^y, V^y , respectively. Further we consider the half-plane of the lattice, $y > a/2$ (the half-plane boundary, $y = a/2$, will be referred to as the crack line since, in the fracture problem, the crack is assumed to be placed at $x < 0, y = a/2$).

The eigensolution bounded in the half-plane is sought in the form

$$w_{n+1}^F = \lambda^n w_1^F, \quad \theta_{n+1}^F = \lambda^n \theta_1^F, \quad n = 1, 2, \dots, \quad |\lambda| \leq 1. \tag{12}$$

It follows from the homogeneous system (10), (11) that

$$\left(\lambda + \frac{1}{\lambda}\right)^2 + b_1 \left(\lambda + \frac{1}{\lambda}\right) + b_2 = 0, \tag{13}$$

$$b_1 = -\frac{6 + 8\cos k - 2\cos^2 k}{\cos k + 2}, \quad b_2 = \frac{16 - 12\cos k + 8\cos^2 k}{\cos k + 2}.$$

Two solutions for $\lambda, |\lambda| \leq 1$, satisfy the above equation

$$\lambda = \lambda_1 \quad \text{and} \quad \lambda = \lambda_2; \quad \lambda_{1,2} = b \pm ic,$$

$$b = \frac{1}{2} \left(\frac{b_1}{2} - \rho \cos \frac{\beta}{2} \right), \quad c = \frac{1}{2} \left(b_3 - \rho \sin \frac{\beta}{2} \right),$$

$$\rho = (b_4^2 + b_1^2 b_3^2)^{1/4}, \quad \beta = \text{Arg}(b_4 + ib_1 b_3), \quad 0 \leq \beta < 2\pi,$$

$$b_3 = \frac{\sqrt{90 + 56\cos k - 2\cos 2k}}{\cos k + 2} \sin^2 \frac{k}{2}, \quad b_4 = \frac{4(\cos 2k - 20\cos k - 29)}{(\cos k + 2)^2} \sin^4 \frac{k}{2}. \tag{14}$$

Substituting this into (10), (12) we obtain the general homogeneous solution for the upper half-plane

$$w_n^F = C_1 \lambda_1^{n-1} + C_2 \lambda_2^{n-1}, \quad n = 1, 2, \dots,$$

$$\theta_n^F = -\lambda_1^{n-1} r(\lambda_1) C_1 - \lambda_2^{n-1} r(\lambda_2) C_2, \quad r(\lambda) = \frac{3(1 - \lambda^2)}{\lambda^2 + 4\lambda + 1}, \tag{15}$$

where $C_{1,2}$ are arbitrary constants.

In addition to this general solution, in the homogeneous fracture problem, we have conditions in the crack region as

$$M(x) = V(x) = 0 \quad (x = -a, -2a, \dots; y = a/2). \tag{16}$$

Hereafter the quantities $M_{m,0}(a/2)$ and $V_{m,0}(a/2)$ are denoted as $M(x)$ and $V(x)$ ($x = am = 0, \pm a, \dots$). Recall that the points at $y = a/2$ correspond to the crack line, that is, they are midpoints of the beams between the nodes at $n=0$ and 1, but not the nodes themselves. The displacements, $w_{m,0}(a/2+0) = w(x)$, and angles, $\theta_{m,0}(a/2+0) = \theta(x)$, are defined by the quantities at $n=1$ as follows:

$$w(x) = w_{m,1} - \frac{a}{2} \theta_{m,1} - \frac{a^2}{48EI} [6M_{m,0}(a) + aV_{m,0}(a)], \tag{17}$$

$$\theta(x) = \theta_{m,1} + \frac{a}{8EI} [4M_{m,0}(a) + aV_{m,0}(a)] \quad (x = 0, \pm a, \dots). \tag{18}$$

Note that we use here notations for the displacements and angles in the beams between the nodes similar to the notations for the forces and moments in (1).

3. The continuous approximation

It can be found from Eqs. (10) and (11), that in the long-wave approximation the lattice corresponds to a continuous anisotropic elastic plate, which transverse displacement, $w(x,y)$, obeys the equation

$$\frac{\partial^4 w(x,y)}{\partial x^4} + \frac{\partial^4 w(x,y)}{\partial y^4} = 0. \tag{19}$$

In the polar coordinate system, $r = \sqrt{x^2 + y^2}$, $\alpha = \arctan(y/x)$, the bending stiffness of the plate

$$D = \frac{EI}{a(|\cos\alpha| + |\sin\alpha|)} \tag{20}$$

is pictured in Fig. 3 as a square with the vertices on the x,y -axes.

Eq. (19) possesses functionally invariant solutions as arbitrary functions of $x \pm \sqrt{\pm i}y$. We choose the solutions that would be far-field asymptotic solutions for the lattice. With this in mind we introduce two square-root type functions

$$\begin{aligned} \Phi_1(x,y) &= \sum_{\nu=0}^3 [-x + y \exp(i\pi(-3/4 + \nu/2))]^{1/2} = \sqrt{2} \left[\sqrt{\sqrt{(x-z)^2 + z^2} - x + z} + \sqrt{\sqrt{(x+z)^2 + z^2} - x - z} \right] \text{sign } y, \\ \Phi_2(x,y) &= \sum_{\nu=0}^3 [-x + y \exp(i\pi(-3/4 + \nu/2))]^{3/2} = -\sqrt{2} [(x-z) \sqrt{\sqrt{(x-z)^2 + z^2} - x + z} \\ &\quad + (x+z) \sqrt{\sqrt{(x+z)^2 + z^2} - x - z}] \text{sign } y - y \left[\sqrt{\sqrt{(x-z)^2 + z^2} + x - z} + \sqrt{\sqrt{(x+z)^2 + z^2} + x + z} \right]. \end{aligned} \tag{21}$$

The functions are defined in the x,y -plane with a branch cut at $y = 0, -\infty < x < 0$; $\Phi_1 > 0, \Phi_2 > 0 (x < 0, y = +0), z = y/\sqrt{2}$.

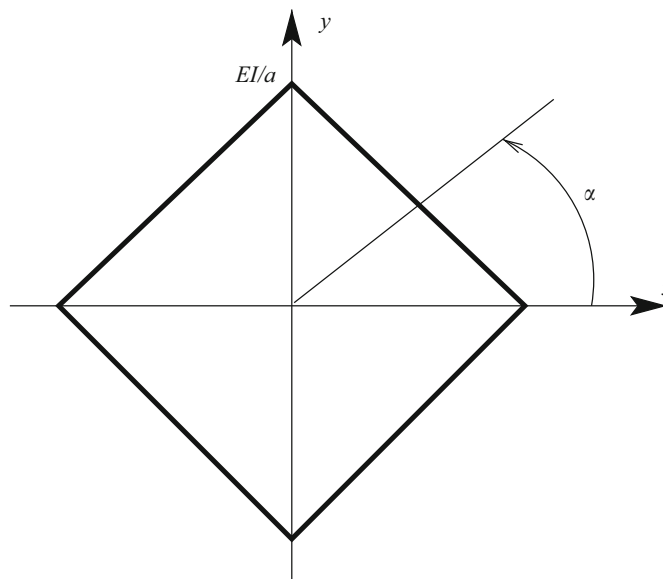


Fig. 3. The bending stiffness of the square lattice related anisotropic plate as a function of the polar angle.

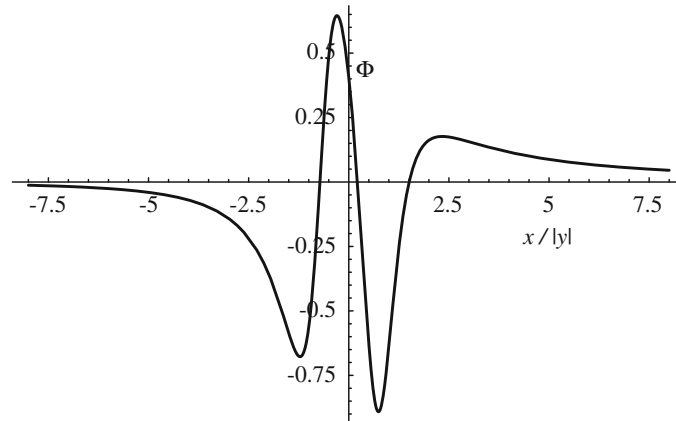


Fig. 4. The prelimiting dependence: the function $\Phi(x/|y|)$ (24).

These representations are valid for $y \neq 0$. The generalized limits at $y = +0$ are

$$\begin{aligned} \Phi_1(x) &= 4x_-^{1/2}, \quad \frac{\partial \Phi_1}{\partial y} = \sqrt{2}x_+^{-1/2}, \quad \frac{\partial^2 \Phi_1}{\partial y^2} = 0, \\ \Phi_2(x) &= 4x_-^{3/2}, \quad \frac{\partial \Phi_2}{\partial y} = -3\sqrt{2}x_+^{1/2}, \quad \frac{\partial^2 \Phi_2}{\partial y^2} = 0, \quad \frac{\partial^3 \Phi_2}{\partial y^3} = \frac{3\sqrt{2}}{4}x_+^{-3/2}, \end{aligned} \quad (22)$$

where the generalized functions can be defined in a more straightforward manner as

$$\begin{aligned} x_{\pm}^{\nu} &= \frac{1}{2} \lim_{y \rightarrow +0} [(\pm x + iy)^{\nu} + (\pm x - iy)^{\nu}], \\ [x_{\pm}^{\nu} &= (\pm x)^{\nu} (\pm x > 0), \quad x_{\pm}^{\nu} = 0 (\pm x < 0), \quad \nu \neq -1, -2, \dots]. \end{aligned} \quad (23)$$

Note that for simplicity the coordinate system for the continuous fields is shifted in such a way that the crack line appears at $y=0$ instead of $y=a/2$ as assumed for the lattice.

The generalized function $x_+^{-3/2}$ is uniquely defined in the Schwartz distribution theory. However, in the considered lattice problem, where we are going to compare the continuous description with the exact one, not only the generalized limit but also the prelimiting function, $\Phi^{(3)}(x,y) \equiv \partial^3 \Phi_2(x,y) / \partial y^3, y \neq 0$, is of interest. For $y \neq 0$ this function can be represented by

$$\Phi_2^{(3)}(x,y) = |y|^{-3/2} \Phi(x/|y|), \quad \Phi(x/|y|) = |y|^{3/2} \Phi_2^{(3)}(x/|y|, 1), \quad q = x/|y| \quad (y \neq 0). \quad (24)$$

Function $\Phi(q)$ is plotted in Fig. 4 (it is the same as $\Phi_2^{(3)}(x/|y|, 1)$).

It can be seen that there is a region where the function takes negative values. This region contracts to the point at the origin, $x=0$, as $y \rightarrow 0$, and it does not support any localized distribution; however, it cannot be neglected. Indeed, although the prelimiting function tends to $x^{-3/2} > 0$ for any $x > 0$, the integral of the former over the x -axis is equal to zero independently of $y \neq 0$. It is worthy to be mentioned, that the transverse force distribution, considered in Section 5 for the antisymmetric mode of the lattice fracture, relates to this prelimiting function.

In connection with the discussed continuous model, we note that the equilibrium equation for the classical bending plate model, $\Delta^2 w = 0$, also possesses functionally invariant solutions. The solutions can be expressed in terms of arbitrary functions of $x \pm iy$ and $y(x \pm iy)$.

Next we consider the lattice with a crack at $m < 0, y=a/2$.

4. Symmetric mode

For the symmetric mode where

$$w_{m,n+1} = w_{m,-n}, \quad \theta_{m,n+1} = -\theta_{m,-n}, \quad (25)$$

in addition to (16), we have

$$\theta(x) = 0, \quad V(x) = 0 \quad (x = 0, a, \dots). \quad (26)$$

Thus $V(x)=0$ over the whole crack line, and this yields a relation between the constants $C_{1,2}$. Indeed, in this case, in view of (18) we have

$$V(x) = V_{m,0}(a) = 0, \quad M(x) = M_{m,0}(a),$$

$$\theta(x) = \theta_{m,1} + \frac{a}{2EI} M(x). \tag{27}$$

On the other hand, referring to (2) and (1), we find that

$$V_{m,0}(a) = \frac{12EI}{a^3} \left[3w_{m,1} - w_{m-1,1} - w_{m+1,1} - w_{m,2} + \frac{a}{2} (\theta_{m,1} - \theta_{m-1,1}^x + \theta_{m+1,1}^x + \theta_{m,2}) \right], \tag{28}$$

$$M_{m,0}(a) = \frac{2EI}{a} \left[\theta_{m,2} + 2\theta_{m,1} - \frac{3}{a} (w_{m,2} - w_{m,1}) \right]. \tag{29}$$

Now, using the Fourier transform and representation (12) we obtain the sought relation between the constants as

$$C_1 p(\lambda_1) + C_2 p(\lambda_2) = 0$$

with

$$p(\lambda) = 2 \frac{\cos k - 3 - \cos^2 k}{\cos k + 2} + 2\lambda + (1 + \lambda)r(\lambda). \tag{30}$$

Thus there remains only one arbitrary constant, say, $C = C_1$.

Referring to (16) and (26), we denote

$$M^F = M_+(k) = \sum_{m=0}^{\infty} M(am) \exp(ikm),$$

$$\theta^F = \theta_-(k) = \sum_{m=-\infty}^{-1} \theta(am) \exp(ikm). \tag{31}$$

Further, using the relations for $M(x)$ (28) and $\theta(x)$ (29), in terms of the Fourier transform, and referring to the mixed boundary conditions (16), (26) we find the connection between $M_+(k)$ and $\theta_-(k)$

$$M_+(k) - \frac{2EI}{a} L(k) \theta_-(k) = 0 \quad (\Im k = 0) \tag{32}$$

with

$$L(k) = \left[1 - \frac{\Im[q(\lambda_1)(1 + \lambda_1)p(\lambda_2)]}{\Im[q(\lambda_2)(1 - \lambda_2)p(\lambda_1)]} \right]^{-1} \quad (\Im k = 0), \tag{33}$$

where p is defined in (30), and

$$q(\lambda) = \frac{3(1 - \lambda)}{\lambda^2 + 4\lambda + 1}, \quad r(\lambda) = \frac{3(1 - \lambda^2)}{\lambda^2 + 4\lambda + 1}. \tag{34}$$

Function $L(k)$ as the kernel of the Wiener–Hopf type equation (32) is presented here in terms of real k . This 2π - periodic function is positive except at zero points $k = 0, \pm 2\pi, \dots$. An asymptote for $k \rightarrow 0$ can be found as

$$L(k) = \frac{|k|}{2\sqrt{2}} + O(k^2). \tag{35}$$

In accordance with the causality principle, we represent this periodic function in the form as

$$L(k) = s_+(k) s_-(k) L_0(k), \quad s_{\pm} = \sqrt{1 - \exp[-(0 \mp ik)]}, \tag{36}$$

where the normalized 2π -periodic function, $L_0(k)$, is positive everywhere on the real k -axis, and the multipliers, s_{\pm} , are regular in the half-planes $\pm \Im k > 0$, respectively (the branch points, $k = \mp 0$, belong to the lower and upper half-plane k , respectively). The related factorization of $L_0(k)$ is achieved using the Cauchy type integral. In this way, we can represent

$$L(k) = L_+(k) L_-(k), \quad L_{\pm}(k) = L_{0\pm}(k) s_{\pm}(k) \tag{37}$$

with

$$L_{0\pm}(k) = \exp \left[\int_{-\pi}^{\pi} \ln L_0(\xi) \delta_{D\pm}(k - \xi) d\xi \right], \tag{38}$$

$$\delta_{D+}(k) = \frac{1}{2\pi} \sum_{m=0}^{\infty} \exp[-(0 - ik)m] = \frac{1}{2\pi} \frac{1}{1 - \exp[-(0 - ik)]},$$

$$\delta_{D-}(k) = \frac{1}{2\pi} \sum_{m=-\infty}^{-1} \exp[(0 + ik)m] = \frac{1}{2\pi} \frac{\exp[-(0 + ik)]}{1 - \exp[-(0 + ik)]}. \tag{39}$$

Now, the Wiener–Hopf equation (32) can be represented as follows:

$$\frac{M_+(k)a}{2EIL_+(k)} - L_-(k)\theta_-(k) = 0. \tag{40}$$

The homogeneous equilibrium equation (32) (or (40)) does not have any nontrivial physically acceptable solution unless the action of the remote load is taken into account. Mathematically, an analytically represented delta-function can reflect that load. This can be done by a vanishing-amplitude distributed load which influence, however, does not vanish, as shown in Slepyan (2002, pp. 401–402). The delta-function can also be introduced directly (see, e.g., Slepyan, 1982, 2005; Mishuris et al., 2009). In doing so we modify (40) as follows:

$$\frac{M_+(k)a}{2EIL_+(k)} - L_-(k)\theta_-(k) = A[\delta_{D+}(k) + \delta_{D-}(k)], \tag{41}$$

where the right-hand side is the analytical representation of the periodically continued generalized function $A\delta(k)$, $A=\text{const}$. This addition is valid since it does not influence the original equilibrium equation (32). Indeed, $L_+(k)$ has a zero at $k=0$, $L_+(k) \sim \text{const} \sqrt{0-ik}$, and returning to (32), that is, multiplying the modified equation (41) by L_+ , we find that the delta function is canceled, and the equilibrium equation (32) remains homogeneous (note that this is true for a specific representation of the delta function as in (41)). At the same time, Eq. (41) gives us a unique, up to an arbitrary multiplier, physically acceptable solution as

$$M_+(k) = \frac{2AEI}{a}L_+(k)\delta_{D+}(k), \quad \theta_-(k) = \frac{A}{L_-(k)}\delta_{D-}(k). \tag{42}$$

The bending moment in the crack front beam, $M(0)$, can be found as follows (see Slepyan, 2002, formulas (2.103), (2.104)):

$$M(0) = \lim_{k \rightarrow i\infty} M_+(k) = \frac{AEIR_1}{\pi a}, \quad R_1 = \exp\left[\frac{1}{\pi} \int_0^\pi \ln L_0(k) dk\right] \approx 0.3216. \tag{43}$$

The distribution of the bending moment and the angle of rotation ahead of and behind the crack front, $m = \pm 1, \pm 2, \dots$, can be obtained by the inverse discrete Fourier transform

$$M(am) = \frac{1}{2\pi} \int_{-\pi}^\pi M_+(k) \exp(-ikm) dk. \tag{44}$$

The same formula can be used for $\theta(am)$.

Note that using the identity

$$\text{Re} \left[\frac{1}{1 - \exp[-i(\xi - k)]} \right] \equiv \frac{1}{2} \tag{45}$$

the function $L_{0+}(k)$ can be expressed in a form more convenient for calculations, namely

$$L_{0+}(k) = L_0(k) \exp(R + iY), \tag{46}$$

$$R = \frac{1}{2\pi} \int_0^\pi \ln \frac{L_0(\zeta)}{L_0(k)} d\zeta, \quad Y = \frac{1}{4\pi} \int_{-\pi}^\pi \cot \frac{k-\zeta}{2} \ln \frac{L_0(\zeta)}{L_0(k)} d\zeta. \tag{47}$$

The results of calculations are presented in Fig. 5 and Table 1.

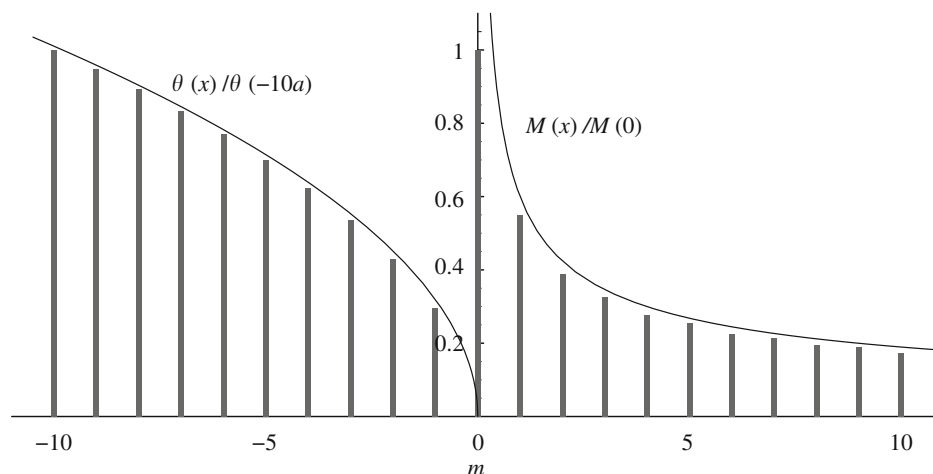


Fig. 5. The bending moments in the beams ahead of the crack, $m \geq 0$, and the rotation angles of the broken beams at $y = a/2 + 0, m < 0$ ($x = am$). Solid lines correspond to the long wave asymptotes for the crack line (49).

Table 1

Moments in the beams in front of the crack and rotation angles of the broken beams at $y=a/2+0$: the lattice solution and the asymptotic values (49).

m	$M(x)/M(0)$	(49)	m	$\theta(x)/\theta(-10a)$	(49)
0	1	∞	0	0	0
1	0.5487	0.5992	-1	0.2968	0.3194
2	0.3892	0.4237	-2	0.4306	0.4518
3	0.3265	0.3459	-3	0.5355	0.5533
4	0.2771	0.2996	-4	0.6233	0.6389
5	0.2543	0.2680	-5	0.7001	0.7143
6	0.2254	0.2446	-6	0.7695	0.7825
7	0.2149	0.2265	-7	0.8331	0.8452
8	0.1941	0.2118	-8	0.8922	0.9035
9	0.1892	0.1997	-9	0.9476	0.9583
10	0.1726	0.1895	-10	1	1.010

In the derived solution, the bending moments are determined for the crack-line beams; however, it cannot be excluded in advance that not the crack-front beam but a different one breaks first. It was shown by numerical analysis of plane problems that crack kinking occurs in a triangular mass–spring lattice under a sufficiently high crack speed (Marder and Gross, 1995) and in hexagonal and square bending beam lattices under the quasi-static crack growth (Ryvkin et al., 2004; Lipperman et al., 2007, 2008). In this connection, the linearly distributed bending moments, $M_{-1,1}^x(x') = M_{-1,0}^x(x')$, in the parallel-to-the-crack-line beams adjacent to the crack-front beam (the beams at $n=0$ and 1 between $m = -1$ and 0) are calculated. It was found that $M_{-1,1}^x(0)/M(0) = 0.2438$ and $M_{-1,1}^x(1)/M(0) = 0.6417$, where $M(0)$ is the bending moment in the crack-front beam. Thus, in the considered problem, no kinking is expected, and the crack resistance analysis can be based on the state of the crack-front beam.

4.1. Long-wave approximation

As the distance from the crack front increases, the lattice solution approaches its long-wave asymptote. The latter follows from (42) as an asymptote for $k \rightarrow 0$

$$M_+(k) \sim \frac{AEI}{a} \frac{L_{0+}(0)}{\pi(0-ik)^{1/2}}, \quad \theta_-(k) \sim -\frac{A}{2\pi L_{0-}(0)(0+ik)^{3/2}}. \tag{48}$$

Consequently, the moment per unit length and the angle are

$$M(x) \sim AEI \frac{L_{0+}(0)}{\pi^{3/2} a \sqrt{ax}} (x \rightarrow \infty), \quad \theta(x) \sim -\frac{A\sqrt{-x/a}}{\pi^{3/2} L_{0-}(0)} (x \rightarrow -\infty), \tag{49}$$

where in accordance with (38)

$$L_{0\pm}(0) = \sqrt{L_0(0)} \mathcal{R}_1^{\pm 1/2} \left(\mathcal{R}_1 = \exp \left[\frac{1}{\pi} \int_0^\pi \ln L_0(k) dk \right] \approx 0.3216, L_0(0) = \frac{1}{2\sqrt{2}} \right). \tag{50}$$

The above-mentioned functionally invariant solutions to Eq. (19) can be used to describe the asymptotic fields in the whole (x,y) -plane ($\sqrt{x^2+y^2}/a \rightarrow \infty$). Based on (21) and (49) we can present the solution as

$$\theta(x,y) \sim -\frac{A}{4\pi^{3/2} \sqrt{a} L_{0-}(0)} \Phi_1(x,y). \tag{51}$$

In these terms,

$$M(x,y) = -EI \frac{\partial \theta(x,y)}{\partial y}, \quad V(x,y) = \frac{\partial M(x,y)}{\partial y}. \tag{52}$$

In the limit, $y \rightarrow +0$, the latter being considered as a generalized function is equal to zero, while the angle and moment asymptotically coincide with those derived for the lattice. At the same time this solution satisfies the equilibrium equation (19) as the long-wave asymptote of the lattice equilibrium equation. Thus, solution (51), (52) does represent the long-wave asymptote of the lattice solution. Comparative plots are presented in Fig. 5.

Relations (43), (44) and (49) define the connection between the lattice state and its continuous asymptote in the case of a semi-infinite crack in an unbounded lattice. At the same time, a difference between these two descriptions is essential only in a close vicinity of the crack front. It follows that the connection is still valid for finite lattice sizes, crack lengths and load parameters if the sizes are considerably greater than the lattice cell size. In this case, the above-mentioned relations can be used for the determination of the state of the crack-front beam based on the crack-front asymptote of the continuous description. In particular, for a finite crack, $-l < x < l$, in the lattice subjected to a uniformly distributed bending

moment, M_∞ , at infinity, $y = \pm \infty$, the continuous solution can be found as

$$\theta(x,y) = -\frac{M_\infty}{\sqrt{2EI}} \Re \left[\sqrt{l^2 - (x + \sqrt{iy})^2} + \sqrt{l^2 - (x - \sqrt{iy})^2} \right],$$

$$M(x,y) = -EI \frac{\partial \theta}{\partial y} = \frac{M_\infty}{\sqrt{2}} \Re \left[\frac{-\sqrt{i}(x + \sqrt{iy})}{\sqrt{l^2 - (x + \sqrt{iy})^2}} + \frac{\sqrt{i}(x - \sqrt{iy})}{\sqrt{l^2 - (x - \sqrt{iy})^2}} \right]. \quad (53)$$

For the crack line, $y = \pm 0$, the finite-crack-associated values are

$$\theta(x, \pm 0) = \mp \frac{\sqrt{2}M_\infty}{EI} \sqrt{l^2 - x^2} H(l^2 - x^2), \quad M(x, \pm 0) = M_\infty \frac{|x|H(x^2 - l^2)}{\sqrt{x^2 - l^2}}, \quad (54)$$

where H is the Heaviside step function, while $V(x, \pm 0) = 0$. Note that we here break the vanishing stress condition; however, if θ is changed to

$$\theta = -\frac{M_\infty}{\sqrt{2EI}} \Re \left[\sqrt{l^2 - (x + \sqrt{iy})^2} + \sqrt{l^2 - (x - \sqrt{iy})^2} - (x + \sqrt{iy}) + (x - \sqrt{iy}) \right], \quad (55)$$

then there is the uniformly distributed moment on the crack faces but not at infinity—as usual in fracture mechanics. The continuous asymptote for the displacement follows from (51) and (21)

$$w(x,y) \sim -\frac{A}{6\pi^{3/2}\sqrt{a}L_{0-}(0)} \Phi_1^{(-1)},$$

$$\Phi_1^{(-1)} = \sum_{\nu=0}^3 [-x + y \exp(i\pi(-3/4 + \nu/2))]^{3/2} \exp(-i\pi(-3/4 + \nu/2)). \quad (56)$$

The lattice under the symmetric bending is pictured in Fig. 6.

4.2. Crack resistance

The critical strain energy of the bond deformed by a uniformly distributed bending moment is

$$U_c = \frac{M^2(0)a}{2EI} = \frac{A^2EI\mathcal{R}_1^2}{2\pi^2 a}. \quad (57)$$

Hence the ‘local’ energy release rate is

$$G_0 = \frac{U_c}{a} = \frac{A^2EI\mathcal{R}_1^2}{2\pi^2 a^2}. \quad (58)$$

The energy release rate on the macrolevel is defined by formula (1.42) in Slepyan (2002) in terms of the long-wave asymptotes (48) (also see (50)), namely, in terms of the asymptotes of $M_+(k)/a$ and $-\theta_-(k)$ for $k \rightarrow 0$. The latter quantities constitute the energy pair similar to the stress and displacement vectors in elasticity. Thus, the ‘global’ energy release

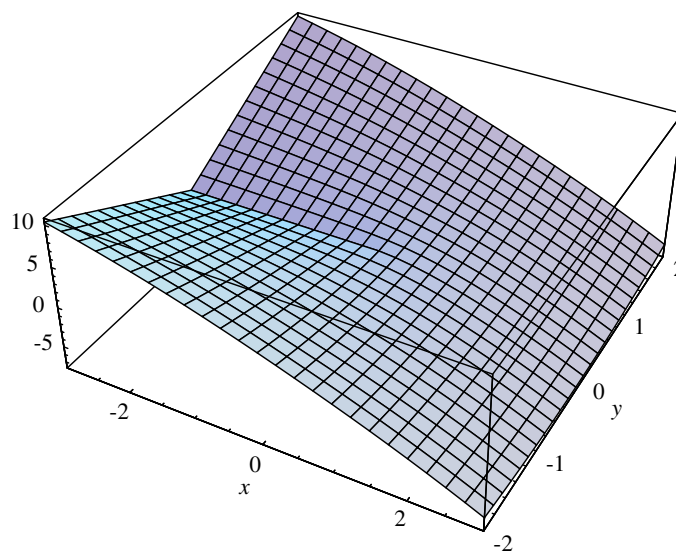


Fig. 6. The lattice under symmetric bending: $w(x,y)/(2A)$ (56).

rate, G , is

$$G = -\lim_{s \rightarrow \infty} s^2 M_+(is) \theta_-(is) / a = \frac{A^2 EI \mathcal{R}_1}{2\pi^2 a^2}, \quad (59)$$

and the energy release ratio is

$$\frac{G_0}{G} = \mathcal{R}_1 \approx 0.3216. \quad (60)$$

This result evidences that approximately $\frac{1}{3}$ of the global energy release is spent on the bond breakage, i.e., on the fracture itself, while $\frac{2}{3}$ of the energy is lost. The latter, in fact, is the energy of oscillations which cannot be seen in the framework of the static formulation. Note that in the case of mode III mass–spring square lattice, the related energy release ratio is $G_0/G = \sqrt{2}-1 \approx 0.4142$ (Slepyan, 2002, p. 505).

The energy release ratio is thus independent of the beam bending stiffness and of the lattice cell size. However, the energy release itself does depend on these quantities. Let $M=M_c$ be the critical bending moment of the beam. It follows from (57) and (59) that $A = \pi a M_c / (EI \mathcal{R}_1)$ and

$$G = \frac{M_c^2}{2EI \mathcal{R}_1}. \quad (61)$$

Lastly, in the case of a geometrically similar structures made of the same material, $M_c = \text{const} \times a^3 \sigma_c$, $I = \text{const} \times a^4$, and

$$G = \text{const} \times \frac{a^2 \sigma_c^2}{E}, \quad (62)$$

where σ_c is the limiting strength and E is the elastic modulus. Note that in a three-dimensional case, G is proportional to a and not to a^2 . This, of course, follows directly from the dimensional analysis.

The bending moment intensity factor can be introduced in this model as

$$K = \sqrt{GE}. \quad (63)$$

Thus the critical value, $K=K_c$, is

$$K_c = \frac{M_c}{\sqrt{2\mathcal{R}_1 I}} = \text{const} \times a \sigma_c. \quad (64)$$

5. Antisymmetric mode

In the case where the transverse displacements are antisymmetric respective to the crack line

$$w_{m,n+1} = -w_{m,-n}, \quad \theta_{m,n+1} = \theta_{m,-n}, \quad (65)$$

conditions (16) on the crack line at $m < 0$ remain valid, while ahead of the crack we have

$$w(x) = 0, \quad M(x) = 0 \quad (x = 0, a, \dots). \quad (66)$$

Thus, in this case, $M(x)=0$ on the whole crack line, and in accordance with (17), (18), the forces and displacements are

$$V(x) = V_{m,0}(a) = -\frac{2}{a} M_{m,0}(a),$$

$$w(x) = w_{m,1} - \frac{a}{2} \theta_{m,1} + \frac{a^3}{24EI} V_{m,0}(a), \quad (67)$$

$$\theta(x) = \theta_{m,1} - \frac{a^2}{8EI} V_{m,0}(a) \quad (x = 0, \pm a, \dots). \quad (68)$$

The solution procedure is similar to the one used in the symmetric case; however, some points are different. The expressions in (15) are still valid, but the coefficients in the relation (30) are now defined by a different relation, namely

$$p(\lambda) = \frac{\lambda^3 - 9\lambda^2 - 9\lambda - 7}{\lambda^2 + 4\lambda + 1} + \frac{10 + 2\cos k}{2 + \cos k}. \quad (69)$$

Consequently, referring to the conditions (16), (66) we come to the following equation with respect to “+” and “–” functions defined similarly to (31)

$$V_+(k) - \frac{24EI}{a^3} L(k) w_-(k) = 0 \quad (\Im k = 0) \quad (70)$$

with

$$L(k) = \left[1 - 4 \frac{\Im[p(\lambda_1) q_1(\lambda_2)]}{\Im[p(\lambda_2) q_2(\lambda_1)]} \right]^{-1}. \quad (71)$$

Here

$$q_1(\lambda) = -\frac{\lambda^2 - 8\lambda - 5}{2(\lambda^2 + 4\lambda + 1)},$$

$$q_2(\lambda) = \frac{2(\cos^2 k - \cos k + 3)}{2 + \cos k} + \frac{\lambda^3 - 5\lambda^2 - 5\lambda - 3}{\lambda^2 + 4\lambda + 1}. \quad (72)$$

As in the symmetric case, the kernel $L(k)$ of the Wiener–Hopf equation (70) is 2π -periodic and positive except for the zero points $k = 0, \pm 2\pi, \dots$. However, the order of zeros is different since for $k \rightarrow 0$

$$L(k) = \frac{|k|^3}{24\sqrt{2}} + O(k^4). \quad (73)$$

Similar to the symmetric case, in accordance with the causality principle, we represent

$$L(k) = s_+(k)s_-(k)L_0(k), \quad s_{\pm} = (1 - \exp[-(0 \mp ik)])^{3/2}, \quad (74)$$

where the normalized 2π -periodic function, $L_0(k)$, is positive everywhere on the real k -axis, and the multipliers, s_{\pm} , are regular in the half-planes $\pm \Im k > 0$, respectively (the branch points, $k = \mp 0$, belong to the lower and upper half-plane k , respectively). The related factorization of $L_0(k)$ is achieved using the Cauchy type integral. Thus

$$L(k) = L_+(k)L_-(k), \quad L_{\pm}(k) = L_{0\pm}(k)s_{\pm}(k) \quad (75)$$

with

$$L_{0\pm}(k) = \exp \left[\int_{-\pi}^{\pi} \ln L_0(\zeta) \delta_{D\pm}(k - \zeta) d\zeta \right]. \quad (76)$$

Eq. (70) can now be rewritten in the form similar to that in (40)

$$\frac{a^2}{24EIL_+(k)} V_+(k) - \frac{L_-(k)}{a} w_-(k) = 0. \quad (77)$$

In contrast to the symmetric case, the higher order zero of $s_+(k)$ allows not only for the delta function but also for its derivative to be introduced in the right-hand side of the equation. The above equation can thus be modified as

$$\frac{a^2}{24EIL_+(k)} V_+(k) - \frac{L_-(k)}{a} w_-(k) = A[\delta_{D+}(k) + \delta_{D-}(k)] + B \left[\frac{d\delta_{D+}(k)}{dk} + \frac{d\delta_{D-}(k)}{dk} \right]. \quad (78)$$

However, the solution corresponding to the B -term does not satisfy the vanishing stress condition. The only physically acceptable solution follows as

$$V_+(k) = \frac{24EIA}{a^2} \delta_{D+}(k)L_{0+}(k)s_+(k), \quad w_-(k) = -\frac{aA\delta_{D-}(k)}{L_{0-}(k)s_-(k)},$$

$$L_{0\pm}(k) = \exp \left[\int_{-\pi}^{\pi} \ln L_0(\zeta) \delta_{D\pm}(k - \zeta) d\zeta \right]. \quad (79)$$

The transverse force in the crack front beam, $V(0)$, is equal to the limit as

$$V(0) = \lim_{k \rightarrow i\infty} V_+(k) = \frac{12EIA\mathcal{R}_2}{\pi a^2}, \quad \mathcal{R}_2 = \exp \left[\frac{1}{\pi} \int_0^{\pi} \ln L_0(k) dk \right] \approx 0.0303. \quad (80)$$

We now find the transverse force distribution on the crack line ahead of the crack, $m = 1, 2, \dots$. Recall that the inverse transform of a function regular in the upper half-plane k , $M_+(k)$ or $V_+(k)$, can be performed in two ways. One is the use of the integral formula (44). The other is shown in Slepyan (2002, Section 2.4.2). In fact, the latter way is the representation of the Fourier discrete transform as a series expansion by $S = \exp(ik)$

$$V_+(k) = \sum_{m=0}^{\infty} V(am) \exp(ikm). \quad (81)$$

Clearly, the series converges in the half-plane $\Im k > 0$, and the coefficients represent the transverse force distribution. The expression for $V_+(k)$ given in (79) expanded as a power series by S is

$$V_+(-i \ln S) = \frac{12EI}{\pi a^2} \sum_{m=0}^{\infty} c_m S^m \exp \left[\sum_{j=0}^m r_j S^j \right], \quad (82)$$

$$c_0 = 1, \quad c_1 = -\frac{1}{2}, \dots, c_m = \frac{(2m-3)!!}{2m!!}, \quad r_j = \frac{1}{\pi} \int_0^{\pi} \cos jk \ln L_0(k) dk. \quad (83)$$

The coefficients $V(am)$ in (81) were obtained by the use of symbolic computation. The normalized forces $V(ma)/V(0)$ in the beams ahead of the crack, $m=0, \dots, 10$, are presented in Fig. 7, where the solid line corresponds to the asymptotic solution (86).

Referring to (74) and (79) we note that the transverse force on the crack line is self-equilibrated

$$\sum_{m=0}^{\infty} V(am) = V_+(0) = 0. \tag{84}$$

That is in accordance with the above force distribution.

As in the symmetric case, we have calculated the linearly distributed moments in the parallel-to-the-crack-line beams at the crack front. The result is as follows: $M_{-1,1}^x(0)/M_0=0.5247$, $M_{-1,1}^x(a)/M_0=0.8843$, where $M_0=V(0)a/2$ is the maximal moment in the crack-front beam. Thus no kinking is expected in the antisymmetric case as well, and the crack resistance can be calculated based on the latter bending moment, M_0 .

It is of interest that, in this mode of fracture, only the crack-front beam resists to the crack advance, whereas the other beams on the crack line ahead of the crack facilitate the fracture. Such type of moment distribution is a result of the scissors-type deformation, Fig. 8, where the opposite displacements of the crack ‘faces’ lead to a rotation around the crack-front beam. Further, it follows from (74) and (79) that $V(k)=0$ at $k=0$, and hence the transverse forces acting on the lattice half-plane are self-equilibrated. In turn, it follows that if the lattice with the crack is deformed by a couple of remote transverse forces applied to the crack face nodes, the value of the force is zero. The corresponding pre-limiting state can be envisioned as that where the forces are applied at a finite distance from the crack front. Under the condition of a fixed transverse force in the crack-front beam, the external forces decrease and vanish as the distance increases and tends to infinity. It can be seen below that the transverse force distribution is still self-equilibrated in the continuous approximation as well.

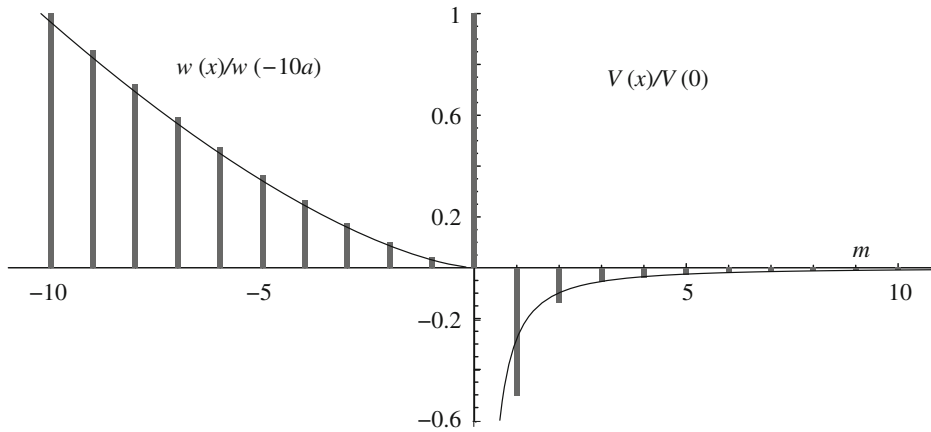


Fig. 7. The transverse forces in the beams ahead of the crack, $m \geq 0$, and the displacements of the broken beams at $y = a/2 + 0, m < 0$ ($x = am$). Solid lines correspond to the long wave asymptotes for the crack line (86).

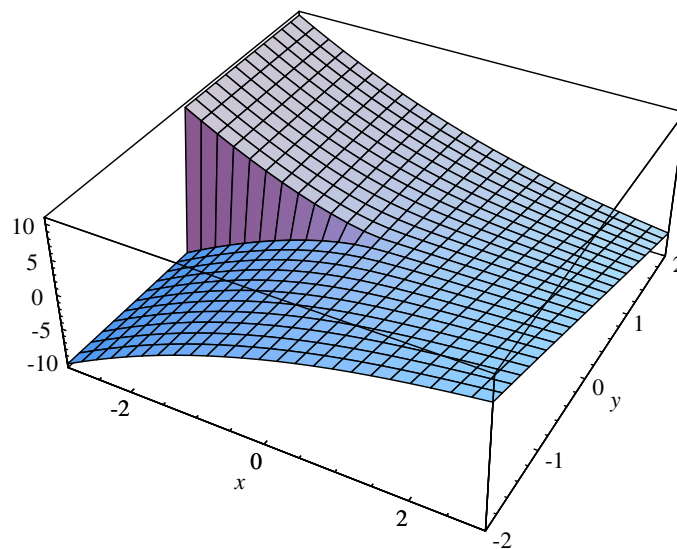


Fig. 8. The lattice under the antisymmetric bending: $w(x,y)/(2A)$ (87).

5.1. Long-wave asymptote

The approximation follows from (79) as the asymptote for $k \rightarrow 0$

$$\begin{aligned}
 V_+(k) &\sim \frac{12AEI\sqrt{\mathcal{R}_2}}{\pi a^2} \sqrt{L_0(0)} \sqrt{0-ik} \quad (k \rightarrow 0), \\
 w_-(k) &\sim -\frac{aA\sqrt{\mathcal{R}_2}}{2\pi\sqrt{L_0(0)}} (0+ik)^{-5/2} \quad (k \rightarrow 0), \\
 \mathcal{R}_2 &= \exp\left[\frac{1}{\pi} \int_0^\pi \ln L_0(k) dk\right] \approx 0.0303, \quad L_0(0) = \frac{1}{24\sqrt{2}}.
 \end{aligned} \tag{85}$$

The inverse transform results in the following expressions for the transverse force per unit length and the displacement on the crack line ($y=a/2+0$)

$$\begin{aligned}
 V(x) &\sim -\frac{6AEI\sqrt{\mathcal{R}_2}L_0(0)}{\pi^{3/2}a^2} \left(\frac{x}{a}\right)^{-3/2} \quad (x \rightarrow \infty), \\
 w(x) &\sim -\frac{2aA\sqrt{\mathcal{R}_2}}{3\pi^{3/2}\sqrt{L_0(0)}} \left(-\frac{x}{a}\right)^{3/2} \quad (x \rightarrow -\infty).
 \end{aligned} \tag{86}$$

As in the symmetric case, the functionally invariant solution (21) can be used for the asymptotic description of the lattice fields in the (x,y) -plane. In accordance with the asymptotes of the solution obtained for the lattice (85), we represent

$$w(x,y) \sim -\frac{A\sqrt{2\mathcal{R}_2}}{6\pi^{3/2}\sqrt{aL_0(0)}} \Phi_2(x,y) \quad (\sqrt{x^2+y^2}/a \rightarrow \infty), \tag{87}$$

where Φ_2 is defined in (21), (22). Asymptotes for the other quantities follow from this as

$$\theta(x,y) = \frac{\partial w(x,y)}{\partial y}, \quad M(x,y) = -EI \frac{\partial \theta(x,y)}{\partial y}, \quad V(x,y) = \frac{\partial M(x,y)}{\partial y}, \tag{88}$$

where the derivatives at $y=+0$ are presented in (22). Recall that the regular function $\Phi_2(x,y)(y \neq 0)$ takes negative values (see Fig. 4), and it can be seen that the asymptotic solution (87) is self-equilibrated as well as the exact solution, namely

$$\int_{-\infty}^{\infty} V(x) dx = 0. \tag{89}$$

We now consider the anisotropic continuous plate with a finite crack, $-l < x < l$, subjected to transverse forces, V_0 , uniformly distributed over the crack faces. Similar to the symmetric case, the finite-crack continuous solution is found to be

$$\begin{aligned}
 w(x,y) &= -\frac{\sqrt{2}V_0}{12EI} \Re[(l^2 - (x + \sqrt{iy})^2)^{3/2} + (l^2 - (x - \sqrt{iy})^2)^{3/2} - (x + \sqrt{iy})^3 + (x - \sqrt{iy})^3], \\
 M(x,y) &= -EI \frac{\partial^2 w(x,y)}{\partial y^2}, \quad V(x,y) = \frac{\partial M(x,y)}{\partial y}.
 \end{aligned} \tag{90}$$

On the crack line it is

$$\begin{aligned}
 w(x, \pm 0) &= \mp \frac{\sqrt{2}V_0}{6EI} (l^2 - x^2)^{3/2} H(l^2 - x^2), \quad M(x, \pm 0) = 0, \\
 V(x, \pm 0) &= V_0 \left[1 + \frac{1}{2} |x|^3 (x^2 - l^2)_+^{-3/2} - \frac{3}{2} |x| (x^2 - l^2)_+^{-1/2} \right].
 \end{aligned} \tag{91}$$

Discrete and continuous distributions are shown in Fig. 7 and Table 2. The lattice under the antisymmetric bending is pictured in Fig. 8.

5.2. Crack resistance

The critical strain energy of the crack-front beam deformed by a linearly distributed bending moment

$$M_{0,0}(y) = V(0) \left(y - \frac{a}{2}\right), \quad 0 < y < a, \quad M_{0,0}(a) = M_c, \tag{92}$$

and the critical value of the transverse force are

$$U_c = \frac{V^2(0)a^3}{24EI} = \frac{6EIA^2\mathcal{R}_2^2}{\pi^2 a}, \quad V(0) = V_c = \frac{2M_c}{a} = \frac{12EIA\mathcal{R}_2}{\pi a^2}. \tag{93}$$

Table 2

Transverse forces in the beams in front of the crack and displacements of the broken beams at $y=a/2+0$. The lattice solution and the asymptotic values calculated in accordance with (86).

m	$V(x)/V(0)$	(86)	m	$w(x)/w(-10a)$	(86)
0	1	$\pm \infty$	0	0	0
1	-0.5025	-0.2782	-1	0.0401	0.0306
2	-0.1362	-0.0984	-2	0.1004	0.0864
3	-0.0547	-0.0535	-3	0.1762	0.1587
4	-0.0378	-0.0348	-4	0.2649	0.2444
5	-0.0267	-0.0249	-5	0.3647	0.3415
6	-0.0200	-0.0189	-6	0.4746	0.4490
7	-0.0158	-0.0150	-7	0.5936	0.5658
8	-0.0128	-0.0123	-8	0.7212	0.6913
9	-0.0107	-0.0103	-9	0.8568	0.8249
10	-0.0091	-0.0088	-10	1.	0.9661

It follows that the local energy release per unit length is

$$G_0 = \frac{M_c^2}{6EI} = \frac{6EIA^2 \mathcal{R}_2^2}{\pi^2 a^2}. \tag{94}$$

The ‘global’ energy release rate, G , is defined by the same relation as in the symmetric case (60) but with respect to the transverse force–displacement energy pair. Referring to (85) we obtain

$$G = -\lim_{s \rightarrow \infty} s^2 V_+(is) w_-(-is)/a = \frac{6EIA^2 \mathcal{R}_2}{\pi^2 a^2}. \tag{95}$$

Thus, the energy release ratio is

$$\frac{G_0}{G} = \mathcal{R}_2 \approx 0.0303. \tag{96}$$

In the case of a geometrically similar structure made of the same material, $M_c = \text{const} \times a^3 \sigma_c$, $I = \text{const} \times a^4$, and relations (62) and (64) are still valid. It is remarkable that in a quasi-static crack advance under antisymmetric bending only about 3% of the far-field energy release goes to the fracture itself, while the rest disappears.

6. Concluding remarks

In this paper, the crack resistance of the square bending beam lattice is expressed in terms of the limiting bending moment. The relation is based on the solutions derived for the lattice with a semi-infinite initial crack and for the related continuous anisotropic bending plate. The latter solution is defined as a far-field asymptote of the former—in the lattice spacing scale. At the same time, under certain conditions it can be considered as a crack-tip asymptote—in the problem for the plate with a finite crack, whose solution is also presented. The energy release ratio is obtained by comparing the energy release in the continuous model with the critical strain energy of the beam in front of the crack. It appears that the critical strain energy of the beam is only part of the total energy release. For the symmetric bending mode the former is approximately equal to $\frac{1}{3}$ of the latter, whereas the corresponding ratio is about $\frac{3}{100}$ in the antisymmetric case. The rest of the energy goes to oscillations caused by the sudden beam breakage; however, the quasi-static formulation cannot trace this dynamic phenomenon but only the total energy lost.

We should stress that in this paper the crack growth is not considered but only the strength of the lattice with an initial crack. The energy release concerns a single step: from the initial state to the state with the crack-front beam broken. The fact that the crack-front beam is most stressed is valid only for the initial static state. After the first beam failure the crack will grow dynamically, and the dynamic amplification factor will play a crucial role. In addition, in the antisymmetric problem, the crack-front beam is stressed maximally at its ends, and the crack will not grow along the line of symmetry. In statics, however, it does not matter where the crack-line beam breaks since it does not influence the lattice state outside this beam. Thus the mathematical formulation of the considered problems is insensitive to positions of the break points, which form the initial crack; they can be out of the crack line but between the lines $n=0$ and 1.

In the lattice, in contrast to the continuous material, short and long cracks can be distinguished. In other words, the crack resistance expressed in terms of the energy release rate, or the critical bending-moment intensity factor, in the related continuous plate, depends on the crack length. In this connection, it is remarkable that the continuous asymptotes for a semi-infinite crack practically coincide with the discrete lattice distributions beginning from several lattice spacing, a , from the crack front (see Figs. 5 and 7). This suggests that a crack length of several lattice spacing can be considered as large enough, such that the corresponding crack resistance is close enough to that for the semi-infinite crack. Note that in the case of in-plane strain of the lattice, where both bending and tensile deformations of the beams arise, this statement does not hold if the beams are too flexible (Quintana Alonso and Fleck, 2007; Lipperman et al., 2008).

It is of interest that the transverse forces, acting on the lattice half-plane in the antisymmetric case, are self-equilibrated. Hence the remote forces are also self-equilibrated, and if the lattice is deformed by a couple of remote transverse forces, for example applied to the crack faces, then these forces are at zero. It means that, under a fixed state of the crack front beam, the moments applied to the crack faces vanish as the application point moves from the crack front to infinity. This is in contrast to the symmetric case, where the remote moment must compensate for the nonintegrable moment distribution ahead of the crack front.

The transverse force distribution on the crack line in the antisymmetric problem is really striking. The lattice with a crack carries the load by the crack-front beam only. Moreover, the other intact beams on the crack line are stressed by opposite direction forces, and they act as external forces, thus increasing the front beam stress. Note that qualitatively this is in agreement with the hypersingular continuous asymptote in its prelimiting expression, which necessarily must take negative values since the total force is equal to zero. The corresponding region contracts to the crack tip as the coordinate, normal to the crack, tends to zero; however, its influence remains non-negligible (in this connection, see Figs. 4 and 7).

In this paper, the infinite lattice with a semi-infinite crack is considered, and the rotation angles may grow unboundedly with the distance from the crack front. The continuous asymptotic solutions show this more transparently. This fact looks to be in disagreement with the linear theory; however, it does not affect the stress–strain and energy release relations. Only the displacements should be recalculated based on the geometrically nonlinear relations—if the considered lattice is so large that the rotation angles are not small enough.

Recall that in the formulation, the torsional stiffness of the beams was neglected. This simplifies the problem, but limits the admissible set of beam structures. A formulation, in which the torsional stiffness is taken into account, leads to more complicated relations. In particular, the general solution is expressed in terms of three exponents, λ , instead of two (see (14)), and the torsion moments, in addition to the bending moments and the transverse forces, are among the boundary conditions. However, in the symmetric case, the torsion moments on the crack line ahead of the crack are zero due to the symmetry. This allows a single Wiener–Hopf type equation to be derived, which is similar to that considered in this paper but with a different kernel. This more general equation can be resolved in the same way as above.

In addition to this generalization, some other related applications of the technique used in this paper can be envisioned. In particular, fracture of lattices of some different topologies and dynamic fracture of such lattices admit this analytical approach. As to the plane problem for bending beam lattices considered numerically in many works, the use of the Wiener–Hopf technique meets difficulties since the mixed problem leads to a matrix equation. Although the above-considered bending modes differ considerably from the plane ones, the fast conversion of the continuous asymptotic description with the discrete lattice solution, found in the former problems, can be expected to exist in some plane problems as well. This suggests a promising combined analytical–numerical method for the latter ones. In this connection, note the paper by Ashby (1983) with estimations of forces and moments in the crack-front beam based on the analysis of the related continuous model.

Acknowledgement

This research was supported, in part, by The Israel Science Foundation (Grant no. 1354/09).

References

- Ashby, M.F., 1983. The mechanical properties of cellular solids. *Metall. Trans. A* 14A, 1755–1769.
- Choi, S., Sankar, B.V., 2005. A micromechanical method to predict the fracture toughness of cellular materials. *Int. J. Solids Struct.* 42, 1797–1817.
- Fleck, N.A., Qiu, X., 2007. The damage tolerance of elastic-brittle, two dimensional isotropic lattices. *J. Mech. Phys. Solids* 55, 562–588.
- Fuchs, M.B., Ryvkin, M., Grosu, E., 2004. Topological alternatives and structural modeling of infinite grillages on elastic foundation. *Struct. Multidisciplinary Optimization* 26, 346–356.
- Gibson, L.J., Ashby, M.F., 1997. *Cellular Solids, Structure and Properties*. Cambridge University Press, Cambridge.
- Huang, J.S., Gibson, L.J., 1991. Fracture toughness of brittle honeycombs. *Acta Metall. Mater.* 39, 1617–1626.
- Lipperman, F., Ryvkin, M., Fuchs, M.B., 2007. Nucleation of cracks in two-dimensional periodic cellular materials. *Comput. Mech.* 39, 127–139.
- Lipperman, F., Ryvkin, M., Fuchs, M.B., 2008. Fracture toughness of two-dimensional cellular material with periodic microstructure. *Int. J. Fract.* 146, 279–290.
- Lipperman, F., Ryvkin, M., Fuchs, M.B., 2009. Design of crack-resistant two-dimensional periodic cellular materials. *J. Mech. Mater. Struct.* 4, 441–457.
- Maiti, S.K., Ashby, M.F., Gibson, L.J., 1984. Fracture toughness of brittle cellular solids. *Scr. Metall.* 18, 213–217.
- Marder, M., Gross, S., 1995. Origin of crack tip instabilities. *J. Mech. Phys. Solids* 43, 1–48.
- Mishuris, G.S., Movchan, A.B., Slepyan, L.I., 2009. Localised knife waves in a structured interface. *J. Mech. Phys. Solids* 57, 1958–1979, doi: 10.1016/j.jmps.2009.08.004.
- Nuller, B., Ryvkin, M., 1980. On boundary value problems for elastic domains of a periodic structure deformed by arbitrary loads. In: *Proceedings of the State Hydraulic Institute, Energia, Leningrad*, vol. 136, pp. 49–55 (in Russian).
- Quintana Alonso, I., Fleck, N.A., 2007. Damage tolerance of an elastic-brittle diamond-celled honeycomb. *Scr. Mater.* 56, 693–696.
- Ryvkin, M., Fuchs, M.B., Lipperman, F., Kucherov, L., 2004. Fracture analysis of materials with periodic microstructure by the representative cell method. *Int. J. Fract.* 128, 215–221.
- Schmidt, I., Fleck, N.A., 2001. Ductile fracture of two-dimensional cellular structures. *Int. J. Fract.* 111, 327–342.
- Slepyan, L.I., 1981. Dynamics of a crack in a lattice. *Sov. Phys. Dokl.* 26, 538–540.
- Slepyan, L.I., 1982. The relation between the solutions of mixed dynamic problems for a continuous elastic medium and a lattice. *Sov. Phys. Dokl.* 27, 771–772.
- Slepyan, L.I., 2002. *Models and Phenomena in Fracture Mechanics*. Springer, Berlin.
- Slepyan, L.I., 2005. Crack in a material-bond lattice. *J. Mech. Phys. Solids* 53, 1295–1313.